Cationic (Azulene)(diene)rhodium(I) Complexes: Spectroscopic, Dynamic, and Catalytic Properties

by **Andreas Johannes Rippert***, **Dimitri N. Laikov**, and **Hans-Jürgen Hansen**

Organisch-chemisches Institut der Universität Zürich, Winterthurerstr. 190, CH-8057 Zürich

In memoriam Luigi M. Venanzi

New [Rh^I(η^5-azulene)(η^4-diene)][BF_4] complex salts **3**–**5** (diene = 8,9,10-trinorborna-2,5-diene (nbd) and (1*Z*,5*Z*)-cycloocta-1,5-diene (cod)) were synthesized according to a known procedure (*Scheme 1*). All of these complexes show dynamic behavior of the diene ligand at room temperature. In the case of the [Rh^I(η^5-azulene)(cod)]$^+$ complex salts **3** and [Rh^I(η^5-guaiazulene)(nbd)]$^+$ complex salt **4a** (guaiazulene = 7-isopropyl-1,4-dimethylazulene), the coalescence temperature of the ^{1}H-NMR signals of the olefinic H-atoms was determined. The free energy of activation ($\Delta G_T^{\neq}$; *Table 1*) for the intramolecular movement of the diene ligands exhibits a distinct dependency on the HOMO/LUMO properties of the coordinated azulene ligand. The DFT (density-functional theory) calculated $\Delta G_{250}^{\neq}$ values for the internal diene rotation are in good to excellent agreement with the observed ones in CD_2Cl_2 as solvent (*Table 2*). Moreover, the $\Delta G_T^{\neq}$ values can also be estimated in good approximation from the position of the longest-wavelength, azulene-centered UV/VIS absorption band of the complex salts (*Table 2*). These cationic Rh^I complexes are stable and air-resistant and can be used, *e.g.*, as precursor complexes *in situ* in the presence of (*M*)-6,7-bis[(diphenylphosphino)methyl]-8,12-diphenylbenzo[*a*]heptalene for asymmetric hydrogenation of (*Z*)-α-(acetamido)cinnamic acid with ee values of up to 68% (*Table 4*).

1. Introduction. – Some years ago, we reported about the synthesis and characterization of [Rh^I(η^5-azulene)(cod)][BF_4] complex salts **3** (cod = (1*Z*,5*Z*)-cycloocta-1,5-diene; *cf. Table 1*), which showed the azulenes coordinated with their five-membered ring to the metal atom [1]. Their synthesis is easy, and the cationic Rh^I complexes are stable in the solid state, even under normal exposure to air over longer periods of time (several years). There is only one earlier report by *Schrock* and *Osborn* [2], who described the synthesis and characterization of the [Rh^I(η^5-azulene)(nbd)]$^+$ ion **4g** itself. Here, we wish to communicate the successful synthesis of different [Rh^I(η^5-azulene)(nbd)][BF_4] salts **4** (nbd = 8,9,10-trinorborna-2,5-diene) together with those of new [M^I(η^5-azulene)(cod)][BF_4] **3** and **5** (M = Rh or Ir). The spectroscopic data, the fluxional behavior of the dienes cod and nbd in these complexes, structural parameters from DFT (density-functional theory) calculations of some of the complexes, and their potential as precursor complexes in the homogeneous, asymmetric hydrogenation of (*Z*)-α-(acetamido)-cinnamic acid (=(2*Z*)-2-(acetylamino)-3-phenylprop-2-enoic acid) in the presence of (*M*)-6,7-bis[(diphenylphosphino)methyl]-8,12-diphenylbenzo[*a*]-heptalene (={[(*M*)-8,12-diphenylbenzo[*a*]heptalene-6,7-diyl]bis(methylene)}bis[diphenylphosphine]) as new, axially chiral ligand [3] are described.

2. Results and Discussion. – 2.1. *Syntheses.* The new complexes **3**–**5** were synthesized in the same manner as described in [1]. The precursor cations,

$[Rh^I(diene)]^+$ and $[Ir^I(cod)]^+$, were generated in THF from the corresponding dimeric μ-dichloro complexes by addition of $AgBF_4$ (*Scheme 1*). The precipitate of AgCl was removed by filtration, and the corresponding azulenes were added. The $[BF_4]^-$ salts of the (azulene)(diene) complexes were then precipitated as red microcrystalline powders by addition of Et_2O.

Scheme 1

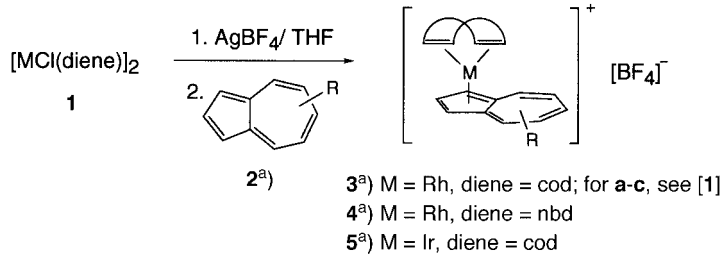

2[a]) **3**[a]) M = Rh, diene = cod; for **a**-**c**, see [**1**]
4[a]) M = Rh, diene = nbd
5[a]) M = Ir, diene = cod

[a]) **a** R = 1,4-Me_2, 7-^{i}Pr
b R = 4,6,8-Me_3
c R = 1,2,3,4,6,8-Me_6
d R = 5,7-Me_2
e R = 5,7-$^i Pr_2$
f R = 4-Me, 7-^{i}Pr
g R = H

2.2. *^{1}H-NMR and UV/VIS Measurements.* The ^{1}H-NMR spectra of the red CD_2Cl_2 solutions of the complexes showed broad and unresolved signals for the olefinic H-atoms, indicating a dynamic exchange process for the H-atom sites in the diene ligands. This exchange process can be explained on the whole by a relative rotation of the cod or nbd ligand around an imaginary diene-Rh-azulene axis with respect to the azulene ligand. The site-exchange process of the olefinic H-atoms of the cyclodiene ligands is displayed schematically in *Scheme 2*. Such dynamic behavior has been proposed for many other transition-metal complexes with cod as ligand (*cf.* [4] and lit. cit. therein). The main structural difference between cod and nbd as ligands has its root in the skeletal flexibility of the former that allows the adoption of chiral conformations also in the complexes (*cf.* [1]) and the complete skeletal rigidity of the latter that preserves its local C_{2v} symmetry in the complexes (see below).

Scheme 2

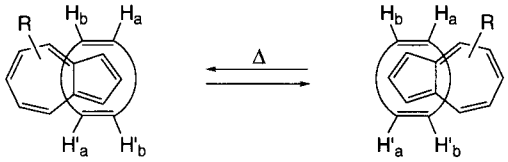

To get more insight into the influence of the azulenes of these complexes on the energy barrier of the relative ligand rotations, we studied the coalescence temperature of the signals of the olefinic H-atoms in the ^{1}H-NMR spectra of a number of complexes of type **3** and **4**, and of **5a**. Fortunately, the complexes **3**, **4a**, and **5a** showed ^{1}H-NMR signal coalescence in a routinely accessible temperature range (230–280 K) for CD_2Cl_2

as solvent. The ^{1}H-NMR signals of the nbd ligand of complex **4a** could be resolved in the temperature range up to 210 K. However, the four signals of the olefinic H-atoms and the two signals of the bridge-head H-atoms, caused by the nonsymmetric substitution pattern of the guaiazulene ligand, showed partial overlapping, so that the coalescence of only one pair of signals could be determined reliably (*cf.* below, *Table 1*).

Measuring the ^{1}H-NMR spectra at 210 K, the $[Rh^I(azulene)(cod)]^+$ ions with symmetrically substituted azulenes showed two broad signals for H–C(sp^2) of the cod ligand, whereas those with nonsymmetrically substituted azulenes showed, as mentioned above already for nbd as ligand, four corresponding broad ^{1}H-NMR signals. The coalescence temperatures of 8 Rh^I complexes and of the Ir^I complex **5a** were finally determined. The results are summarized in *Table 1*.

Table 1. *Coalescence Temperature of the ^{1}H-NMR Signals of the Olefinic H-Atoms of the Diene Ligands in Complexes of Type* **3**–**5** *and the Derived Free Energy of Activation*[a]). For the diene ligands and azulene substituents, see *Scheme 1.*

	Coalescence temperature [K]	$k_r(T)$[b]) [s^{-1}]	$\Delta G_T^{\ddagger}$[c]) [$kJ \cdot mol^{-1}$]
3a	255, 271	52.83, 290.45	53.6 (53.7, 53.4)
3b	243	522.90	46.5
3c	234	41.63	49.6
3d	274	93.99	56.6
3e	275	209.17	55.0
3f	259, 279	133.91, 258.60	54.0 (53.4, 54.5)
3g	251	167.72	50.4
4a	230/–[d])	413.19	44.3
5a	254, 255	323.60, 515.73	49.3 (49.7, 48.9)

[a]) $\Delta G_T^{\ddagger} = RT \ln\left(\frac{h \cdot k_r(T)}{k \cdot T}\right)$; $k_r = \frac{\pi \cdot \Delta\nu}{\sqrt{2}}$. [b]) See also *Exper. Part.* [c]) Average $\Delta G_T^{\ddagger}$ values are given in the case of nonsymmetrically substituted azulene complexes; in parentheses, the two single values of $\Delta G_T^{\ddagger}$. Margins of error: ± 5%. [d]) Overlap of signals in the low-temperature ^{1}H-NMR spectrum allowed the determination of only one coalescence temperature (see text).

The variation in the free energy of activation of the different $[Rh^I(azulene)(cod)]^+$ complexes is markedly dependent on the alkyl substitution pattern of the azulene core, accounting for a change in $\Delta G_T^{\ddagger}$ of *ca.* 20%. The lowest $\Delta G_T^{\ddagger}$ value is found for complex **3b** with Me groups at the azulene skeleton at C(4), C(6), and C(8), whereby additional Me groups at C(1), C(2), and C(3) as in complex **3c** do only slightly increase the corresponding $\Delta G_T^{\ddagger}$. This latter observation is also supported by the $\Delta G_T^{\ddagger}$ values of the guaiazulene complex **3a** and its 1-nor derivative **3f**, which differ by less than 1%, far within the range of the margin of error. On the other hand, the highest $\Delta G_T^{\ddagger}$ value is observed for complex **3d**, which possesses Me groups at C(5) and C(7) of the azulene ligand. In accordance with this finding is the comparable $\Delta G_T^{\ddagger}$ value that is met with complex **3e**, which carries ^{i}Pr groups instead of Me groups at C(5) and C(7). In this way, the variance in the $\Delta G_T^{\ddagger}$ values resembles *Plattner*'s displacement rule for the longest-wavelength electronic absorption band of substituted azulenes [5], which is dependent on the HOMO/LUMO splitting caused by the substitution pattern of the azulenes (*cf.* [6]). Indeed, one also finds for the complex cations a long-wavelength ligand-centered

absorption that can be attributed to the coordinated azulenes (*Table 2*). In comparison to the free azulenes (*cf.* [5][6]), it appears, however, as expected at distinctly shorter wavelengths. Moreover, the wavenumber ($1/\lambda$) of this band, by omission of the data of the heavily substituted complex **3c**, correlates linearly quite well with the measured $\Delta G_T^{\neq}$ values, leading to $\Delta G_T^{\neq} = 354.22 - 1.554 \cdot 10^5/\lambda$ ($r^2 = 0.891$). The $\Delta G_T^{\neq}$ values, calculated with this equation on the basis of the observed position of the azulene-centered absorptions for the cod complexes **3** are also listed in *Table 2*. Larger deviations from the observed $\Delta G_T^{\neq}$ values are only found for complexes **3f** and **3g** as well as for the heavily substituted complex **3c**, which was not included in the regression analysis. The equation for the cod complexes also allows to estimate the $\Delta G_T^{\neq}$ values of the nbd complexes **4** on the basis of the λ_{max} value of the azulene-centered electronic transition of these complexes (*cf. Table 2*). The $\Delta G_{230}^{\neq}$ of 44.3 kJ/mol determined for **4a** and the calculated one of 39.2 kJ/mol, which is less than 12% lower, indicate the reliability of such estimates for the nbd complexes **4**.

Table 2. *Longest-Wavelength Azulene-Centered VIS Absorptions of the [M^I(η^5-azulene(diene)]$^+$ Ions together with Observed and Calculated ΔG$^{\neq}$ Values of Azulene–Diene Rotation*[a]). For the diene ligands and azulene substituents, see *Scheme 1.*

	λ_{max} [nm]	log ε	$\Delta G_T^{\neq}$ [kJ·mol^{-1}]	$\Delta G_T^{\neq}$ (reg) [kJ·mol^{-1}]	$\Delta G_{250}^{\neq}$ (DFT)[b]) [kJ·mol^{-1}]
3a	517.1	3.73	53.6	53.7	–
4a	493.3	3.53	44.3	39.2	–
5a	538.0	3.68	49.3	–	–
3b	505.6	3.78	46.5	46.7	45.9
4b	499.6	3.64	–	43.2	–
3c	516.6	3.82	49.6	53.4	–
3d	522.8	3.79	56.6	57.0	57.2
4d	492.8	3.67	–	38.9	–
3e	518.8	3.81	55.0	54.7	–
3f	514.0	3.83	54.0	51.9	51.3, 50.5
3g	514.7	3.63	50.8	52.3	53.1 (52.4)[c])
4g	–	–	–	–	41.0

[a]) $[BF_4]^-$ salts in CH_2Cl_2; for coalescence temperatures, see *Table 1*. [b]) $\Delta G_T^{\neq}$ values according to DFT calculations (see text and *Exper. Part*). [c]) In parentheses, $\Delta G_{250}^{\neq}$ based on relativistic electronic-energy calculations with nonrelativistic vibrational contributions.

The experimental results clearly demonstrate that the character of the cations of complexes **3**–**5** is mainly determined by the $HOMO_{azulene}$ interaction with the corresponding electrophilic [M^I(η^4-diene)]$^+$ fragment. The alkyl-substituent effects on the position of the longest-wavelength azulene-centered electronic transition of the azulenes as well as on the $\Delta G^{\neq}$ values of the azulene-diene rotation are in full agreement with the orbital symmetry of the HOMO and LUMO of azulene (see, *e.g.*, [7]). In this way, the internal rotation in the complexes **3**–**5** can be understood as a circular motion of the η^5-coordinated azulenes around a common axis with the fixed [M^I(η^4-diene)]$^+$ fragment.

2.2. *DFT Calculations.* We tried to get more insight into the ground- and transition-state structures of the azulene-diene rotation of the Rh-complex ions of **3** and **4** by DFT calculations (for details see *Exper. Part*). Some of the relevant calculated data are listed in *Tables 2* and *3*. The calculated $\Delta G^{\ddagger}$ values for 250 K as medium temperature of the ^{1}H-NMR experiments are in good to very good agreement with those derived from the coalescence measurements in the range of 230 to 280 K. Indeed, they correlate much better with $\Delta G_T^{\ddagger}$ (reg), especially for complexes **3f** and **3g**. The presence of Rh^I in the complexes, which is much heavier than the C- and H-atoms, causes relativistic effects (*cf.* [8]). However, the calculated relativistic $\Delta G_{250}^{\ddagger}$ value for the azulene-diene rotation of the unsubstituted azulene complex **3g** lies only slightly below (1.4%) the non-relativistic value. The corresponding structural data of **3g** match very well with those of the X-ray analysis of **3a** (*Table 3*), especially for the cod part. The deviation of $< 1.3\%$ for the azulene part may be the result of the substituent effects of **3a**. However, the calculated structural parameters (*Table 3*) for the ground states of the investigated complexes are all very similar. The average interatomic Rh–C distances of the cod part are close to those from the X-ray crystal-structure analysis of **3a** (deviation $< 1\%$), and also the deviations of the Rh–C distances of the azulene part do not exceed 3%. Guaiazulene (**2a**) and 7-isopropyl-4-methylazulene (**2f**) form with the [Rh^I(η^4-cod)]$^+$ ion diastereoisomeric complexes, because the cod ligand adopts a (*P*,*P*)- or (*M*,*M*)-conformation as in its noncomplexed state[1]). The calculated structural parameters are, as expected, very similar for the pair of diastereoisomeric complexes of **3a** and **3f**. In these cases, the azulene-diene rotation is superimposed with the thermal epimerization of the diastereoisomeric complexes. The DFT calculations for **3f** indicate that $\Delta G^{\ddagger}$(epimerization) amounts only to a forth of $\Delta G^{\ddagger}$(rotation) (*cf. Fig. 1*). In the ground-state structure of the complexes **3**–**5**, the C=C bonds of the diene ligands are oriented parallel to the longitudinal axis of the azulenes (*cf. Fig. 2*), so that in the cod complexes the two synclinal ethane-1,2-diyl fragments with (*P*,*P*)- or (*M*,*M*)-configuration are placed above C(3a)–C(8a) and C(2), respectively, of the azulene part. This situation allows the formation of two diastereoisomeric transition states of epimerization, which differ in $\Delta G_{250}^{\ddagger}$ by only 1 kJ/mol in favor of the (S_p,*P*,*M*) transition state[2]).

The transition-state structures of the azulene-diene rotation are characterized by a 90° circular movement, so that now the two C=C bonds of the diene ligands are situated above C(2) and C(3a)–C(8a), respectively, of the azulene part. This situation is displayed in *Fig. 2* for the cationic [Rh^I(cod)(5,7-dimethylazulene)] complex **3d**. A comparison of the calculated ground-state and transition-state structures of the Rh^I complexes (*cf. Table 3*) reveals that in going from the ground to the transition state, the average lengths of the Rh–C bonds of the azulene part are elongated, and at a similar

---

[1]) Indeed, both complex forms of **3a** were found in the X-ray crystal-structure analysis of **3a** (*cf.* [1] and below). See [9] for experimental data of cod and [10] for calculations of its conformational space.

[2]) The Rh-atom was taken as reference atom to assign the stereodescriptor for the plane of chirality of the azulene part, given by the clockwise (R_p) or counter-clockwise (S_p) arrangement of the first three C-atoms (C(1),C(2),C(3)) of the azulene core. The stereodescriptors of the helical chirality of the cod ligand refer to the ethane-1,2-diyl moieties above C(2) (first) and C(3a)–C(8a) (second), respectively, of the azulene ligand.

Table 3. *Some Relevant DFT-Calculated Data of the Internal Azulene–Diene Rotation in the [Rh^{I}(η^5-azulene)(η^4-diene)]$^+$ Complex Ions*[a])

	Substituents at the azulene part	Diene	Ground state			Transition state		
			d_1 [pm]	d_2 [pm]	B(diene) [°]	d_1 [pm]	d_2 [pm]	Θ(diene) [°]
3a	1,4-Me_2, 7-^{i}Pr	cod	232.6	220.4	33.9, 33.3	–	–	–
			(226.3)	(218.5)	(35, 34)			
			232.9	220.3	−33.6, −32.9	–	–	–
3b	4,6,8-Me_3	cod	233.3	219.5	33.0, 32.7	238.8	215.1	29.3, 30.6
3d	5,7-Me_2	cod	232.9	220.7	34.0, 33.4	240.7	215.0	28.9, 30.7
3f	4-Me, 7-^{i}Pr	cod	233.0	220.1	33.7, 33.2	240.0	215.0	29.0, 30.6
			233.1	220.1	−33.3, −33.0	239.9	215.0	−29.3, −30.1
3g	H[b])	cod	233.0	220.2	34.4, 33.5	240.7	215.3	29.2, 30.9
			229.7	218.4	34.0, 33.5	236.1	213.6	29.3, 31.2
			242.5	219.1	33.5, 32.6	240.4	214.8	28.0, 30.8
4g	H	nbd	232.3	218.9	–	239.0	214.5	–
–	[c])	cod	–	210.6	30.5/30.6	–	–	–

[a]) If not otherwise stated, the counterion ($[BF_4]^-$) and the solvent (CD_2Cl_2) were not taken into account; d_1 = average Rh-azulene (C(1,2,3,3a,8a)) distance, d_2 = average Rh–C(sp^2) distance of the diene, and Θ(diene) = torsion angles at the C(sp^3)–C(sp^3) bond of the cod ligand. Data from the X-ray structure analysis of **3a** [1] in parentheses. [b]) Second line: values of a relativistic calculation; third line: values for the ion pair with $[BF_4]^-$ as counterion (for details see text). [c]) Values for the fragment [Rh(η^4-cod)]$^+$.

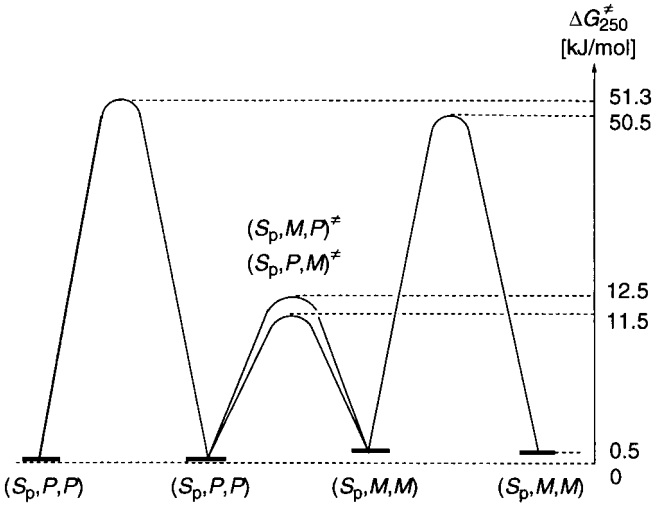

Fig. 1. *Comparison of* ΔG^+ *(rotation) and* ΔG^+ *(epimerization) as obtained by DFT calculations*

extent, those to the diene ligand are shortened. This holds for the cod as well as for the nbd ligand. These observations clearly demonstrate that, indeed, the azulene moiety is turned against the more or less rigid [Rh^{I}(η^4-diene)] fragment to attain the transition state of the azulene-diene rotation. The torsion angles of the cod ligand are slightly reduced by *ca.* 10% in the transition state. A closer look at the structural data discloses

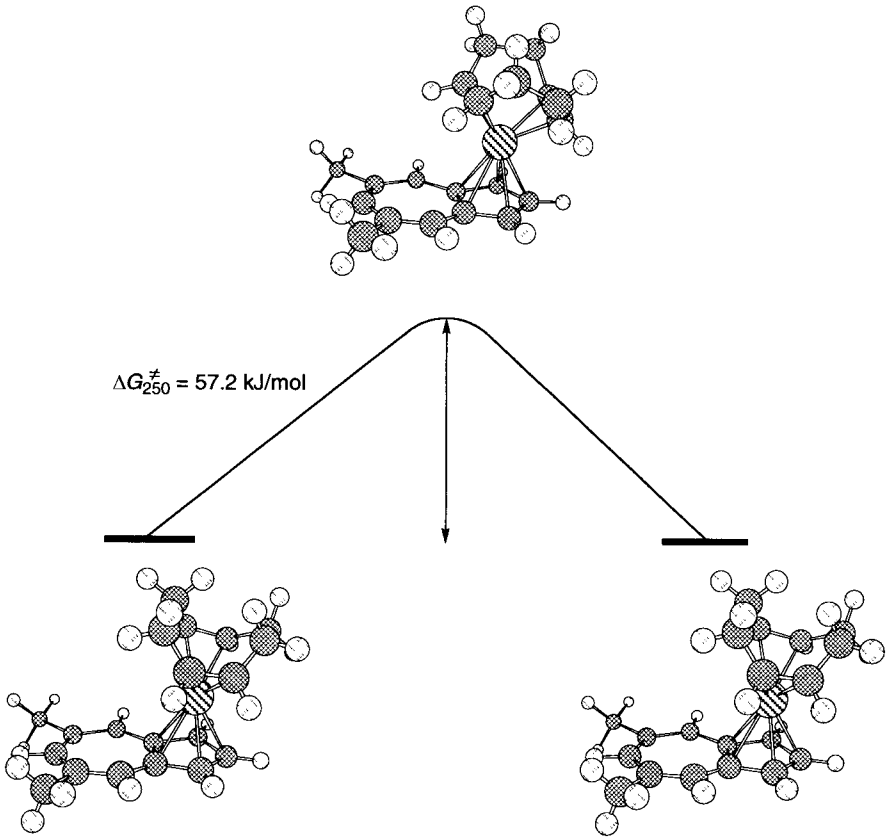

Fig. 2. *DFT Calculated ground-state and transition-state structures for the azulene–cod rotation of the [Rh^{I}(cod)(5,7-dimethylazulene)]$^{+}$ cation of* **3d**

that there are other subtle changes in both ligands around Rh^{+} in going from the ground to the transition state, which may not be regarded as exact measures, but, at least, as recognizable trends. All ground-state structures of the complexes exhibit a distinct pitch of their [Rh^{I}(diene)]$^{+}$ fragment against C(2) of the azulene part, which deviates clearly from the plane of the C-atoms of the five-membered ring, and is most expressed in the [Rh^{I}(cod)]$^{+}$ complex **3d** where it amounts to 2.6 pm away from the Rh-atom (see *Fig. 3*). Complex **3d** exhibits the largest $\Delta G^{\neq}$ value for the azulene-diene rotation, *i.e.*, the strongest bonding between the azulene part and the [Rh^{I}(cod)]$^{+}$ fragment. This deviation is also found in the other complexes, including **4g**, but is slightly diminished, in agreement with the smaller found or calculated $\Delta G^{\neq}$ values for the azulene-diene rotation. The deviation almost vanishes in the transition state of the azulene-diene rotation. In this way, the ground-state structures of the complexes indicate their tendency to be made out of a complexed allyl anion that is 1,3 bridged by a tropylium-like structure (*cf. Fig. 3*). This situation is most clearly pronounced in a specific zwitterionic structure for **3g** with the inclusion of [BF$_4$]$^{-}$ as counterion that we found by

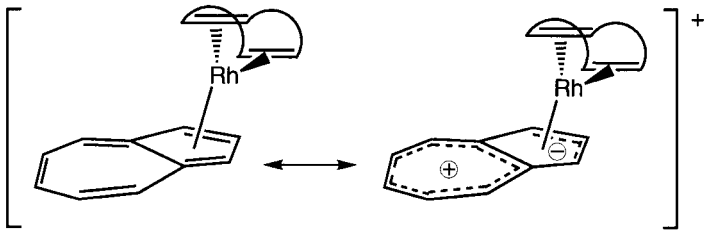

3g or **4g**

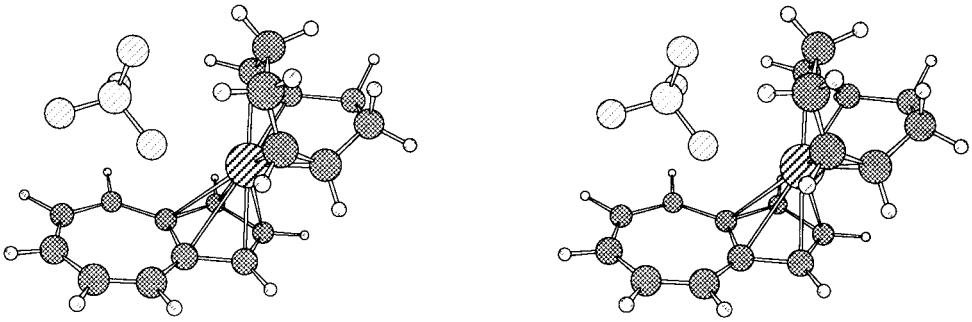

Fig. 3. *DFT Calculated, most stable structure of [Rh^{I}(cod)(azulene)] BF_4* (**3g**) *and postulated resonance structures of* **3g** *and its nbd analogue* **4g**

calculation as the most stable one (*cf. Fig. 3* as well as *Table 3*), and where the anion sits, slightly asymmetrically, above the seven-membered ring of the complexed azulene[3]).

Another feature of the transition-state structures of the cod complexes with symmetrically substituted azulenes is the fact that the cod ligand preserves its twist-boat arrangement with slightly distorted local C_2 symmetry (*cf.* Θ(diene) in *Table 3*). As a consequence, the C=C bond of the cod ligand, which is located above the C(3a) −C(8a) bond, is not in a perfect parallel disposition to this bond or, in other words, the four C-atoms involved deviate from an ideal plane by *ca.* 5 pm. This is in contrast to the corresponding [Rh^{I}(nbd)]$^+$ complex **4g** of azulene, which shows perfect C_s symmetry in its ground- and transition-state geometry of the azulene-diene rotation. Thus, the azulene-cod rotation takes place with retention of the configuration of the cod ligand as

[3]) In the transition state of the azulene-cod rotation of this zwitterions, the $[BF_4]^-$ ion sits beside the cationic complex, whereby the Rh···B interatomic distance increases from 367 pm (ground state) to 445 pm and the closest Rh···F interatomic distance from 262 pm to 381 pm. The calculated $\Delta G^{\neq}_{250}$ value amounts in this case to 45.4 kJ/mol, which is distinctly lower then the observed $\Delta G^{\neq}_{250}$ value. Inclusion of other spatial positions of the counterion $[BF_4]^-$ reduces the $\Delta G^{\neq}_{250}$ values further (*e.g.*, for a start position with $[BF_4]^-$ beside the σ-plane of the azulene ligand, a $\Delta G^{\neq}_{250}$ value of 43.6 kJ/mol was calculated). We conclude from these calculations with inclusion of defined positions of $[BF_4]^-$ that this nonpolarizable anion does not interfere with the azulene-diene rotation in the cationic complexes of type **3**–**5** in CD_2Cl_2 solutions.

we have discussed already (*cf. Fig. 1*). This process is energetically separated from the epimerization or racemization of the cod ligand, which takes place *via* a boat-like arrangement of the cod ligand[4]) already in the ground-state structure of the complexes with $\Delta G^{\neq}$ of only a forth of that of the azulene-diene rotation.

2.3. *Asymmetric Hydrogenations.* We tested the salts **3a**, **4a**, and **4b** as air-stable precursor complexes, which can easily transfer their $[Rh^{I}(diene)]^{+}$ units to chiral bis[diphenylphosphine] ligands, in asymmetric hydrogenations. As chiral ligand, we used (*M*)-6,7-bis[(diphenylphospino)methyl]-8,12-diphenylbenzo[*a*]heptalene, which we have recently synthesized [3], and as substrate (*Z*)-α-(acetamido)cinnamic acid. The hydrogenations were performed at room temperature under a H_2 pressure of 5 atm in MeOH (see *Table 4*). We found enantioselectivities of up to 68%, which are comparable with those reported in [5]. It is remarkable that the crystalline complex salt **3a** proved its activity even after storage for several years under air and normal laboratory conditions. Therefore, the azulene complexes **3** and **4** fulfill the requirements as useful precursor complexes for homogeneous catalysis, *i.e.*, they are air-stable and easy to handle.

Table 4. *Enantioselectivities of the Hydrogenation of* (Z)-α-*(Acetamido)cinnamic Acid with [Rh*[I]*(azulene)(diene)]BF*$_4$ *as [Rh*[I]*(diene)]*$^{+}$ *Source and* (M)*-6,7-Bis[(diphenylphosphino)methyl)]-8,12-diphenylbenzo[*a*]heptalene as Ligand*[a])

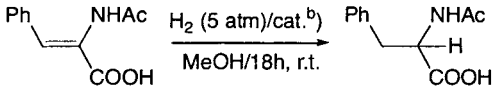

Entry	Catalyst Rh^{I} source	Configuration of ligand	Solvent	ee [%] (config.)
1	$[Rh^{I}(cod)_2]BF_4$	(*P*)	THF	77, 69 (*R*[c])
2	**3a**	(*M*)	MeOH	68 (*S*)
3	**4a**	(*M*)	MeOH	67 (*S*)
4	**4b**	(*M*)	MeOH	65 (*S*)

[a]) Ligand (L) = 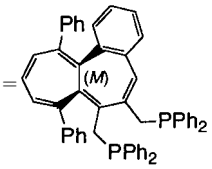

[b]) Cat.: Rh^{I} complex (0.50 mol-%)/L (0.55 mol-%). [c]) Data taken from [3].

We thank our NMR laboratory for specific NMR measurements and our Analytical Laboratory for elemental analyses. We are also thankful to *Xudong Jin* for a sample of the enantiomerically pure (*M*)-heptalene ligand. The financial support of this work by the *Swiss National Science Foundation* is gratefully acknowledged.

---

4) Our DFT calculations of cod itself indicate that the energetically most-favorable conformation is the twist-boat (see [10] for definitions), which is transformed into its mirror image *via* the twist form as transition state, lying 15.5 kJ/mol above the twist-boat conformation. A second, energetically less-favorable pathway for the transformation of the twist-boat conformation of cod into its (*P*,*P*)- and (*M*,*M*)-form *via* the C_s-symmetric half-chair and the C_{2h}-symmetric chair conformation of cod as intermediates can also be involved, whereby the two additional conformations lie 5.4 and 10.0 kJ/mol, respectively, above the twist-boat form of cod.

Experimental Part

1. *General*. See [1][3]. $[Rh^{I}(nbd)Cl]_2$, and $[Ir^{I}(cod)Cl]_2$ were synthesized according to [11–13]. Azulenes **2d** and **2e** were synthesized according to [14]. The source of 7-isopropyl-4-methylazulene (**2f**) was lactaroviolin (*cf.* footnote 2 in [15]), which was hydrogenated and then decarbonylated with $[RhCl(PPh_3)_3]$. The catalytic hydrogenation of (*Z*)-α-(acetamido)cinnamic acid (*Fluka*, *puriss.*) as well as the determination of the ee values and the absolute configuration were performed in analogy to [3]. UV/VIS: $\lambda_{max}(\log \varepsilon)$ in nm, λ_{min} = min.

The DFT calculations were performed with a computer code developed by one of us [16]. The gradient-corrected functional of *Perdew*, *Burke*, and *Ernzerhof* [17] as well as extended basis sets of Gaussian type were used. Full geometry optimization, followed by harmonic vibrational analysis was performed for each of the structures considered with analytically computed first and second derivatives of the energy. The $\Delta G^{\neq}_{250}$ values were calculated in the harmonic approximation.

2. *Synthesis of the Complex Salts.* The procedure as described in [1] was followed; for the salts **3a**–**c**, see [1].

2.1. *Data of the [Rh^{I}(cod)(azulene)] Complex Salts* **3d**–**g**.

[(1,2,5,6-η)-Cycloocta-1,5-diene][(1,2,3,3a,8a-η)-5,7-dimethylazulene]rhodium(1+) Tetrafluoroborate(1−) ($[Rh^{I}(cod)(\eta^5\text{-}5,7\text{-dimethylazulene})][BF_4]$; **3d**): M.p. 235.1–235.7°. UV/VIS (CH_2Cl_2): 522.8 (3.80), 357.2 (sh, 3.59), 343.6 (3.65), 317.2 (4.11), 294.0 (sh, 4.23), 283.6 (4.31); min.: 430.1 (3.33), 354 (3.45), 305.2 (4.06), 253.2 (4.19). ^{1}H-NMR (300 MHz, $CDCl_3$): 7.96 (*s*, H–C(6)); 7.83 (*s*, H–C(4), H–C(8)); 7.10 (superimp. *td*, $^3J(1,2)$ = 3.0, $^2J(2,^{103}Rh)$ = 2.1, H–C(2)); 6.00 (*d*, $^3J(1,2) = {}^3J(3,2)$ = 3.0, H–C(1), H–C(3)); 5.13 (br. *s*, olef. H (cod)); 2.73 (*s*, 2 Me); 2.05 (br. *s*, allyl. H (cod)). Coalescence temp.: 274 K, $\Delta\nu$ = 42.31 Hz. ^{13}C-NMR (75 MHz, $CDCl_3$): 145.3 (*s*, C(5), C(7)); 141.9 (*s*, C(6)); 133.7 (*s*, C(4), C(8)); 114.9 (*d*, $^1J(3a,^{103}Rh) = {}^1J(8a,^{103}Rh)$ = 2.9, C(3a), C(8a)); 104.8 (*d*, $^1J(2,^{103}Rh)$ = 4.5, C(2)); 86.5 (*d*, $^1J(1,^{103}Rh) = {}^1J(3,^{103}Rh)$ = 3.7, C(1), C(3)); 82.1 (*d*, $^1J(C(sp^2;$ cod), $^{103}Rh)$ = 12.1, olefin. C (cod)); 30.4 (*s*, allyl. C (cod)); 27.3 (*s*, 2 Me). Anal. calc. for $C_{20}H_{24}BF_4Rh$ (454.12): C 52.90, H 5.33; found: C 52.71, H 5.59.

[(1,2,5,6-η)-Cycloocta-1,5-diene][(1,2,3,3a,8a-η)-5,7-diisopropylazulene]rhodium(1+) Tetrafluoroborate(1−) ($[Rh^{I}(cod)(\eta^5\text{-}5,7\text{-diisopropylazulene})][BF_4]$; **3e**): M.p. 219.2–220.6°. UV/VIS (CH_2Cl_2): 518.8 (3.81), 355.6 (3.58), 342.0 (sh, 3.64), 317.2 (4.11), 292.4 (4.23), 282.0 (4.31); min.: 430.1 (3.31), 352.4 (3.44), 304.4 (4.05), 290.8 (4.21), 253.2 (4.19). ^{1}H-NMR (300 MHz, $CDCl_3$): 7.98 (br. *s*, H–C(6)); 7.89 (*d*, $^3J(4,6) = {}^3J(8,6)$ = 1.5, H–C(4), H–C(8)); 7.12 (superimp. *td*. $^3J(1,2)$ = 3.0, $^2J(2,^{103}Rh)$ = 2.0, H–C(2)); 6.10 (*d*, $^3J(1,2) = {}^3J(3,2)$ = 3.0, H–C(1), H–C(3)); 5.03 (br. *s*, olef. H (cod)); 3.19 (*sept.*, ^3J = 6.9, 2 Me_2CH); 2.03 (br. *s*, allyl. H (cod)); 1.40 (*d*, ^3J(H,H) = 6.9, 2 Me_2CH). Coalescence temp.: 275 K, $\Delta\nu$ = 94.16 Hz. ^{13}C-NMR (75 MHz, $CDCl_3$): 156.0 (*s*, C(5), C(7)); 137.9 (*s*, C(6)); 132.2 (*s*, C(4), C(8)); 114.8 (*d*, $^1J(3a,^{103}Rh) = {}^1J(8a,^{103}Rh)$ = 3.0, C(3a), C(8a)); 104.4 (*d*, $^1J(2,^{103}Rh)$ = 4.6, C(2)); 87.4 (*d*, $^1J(1,^{103}Rh) = {}^1J(3,^{103}Rh)$ = 3.8, C(1), C(3)); 81.0 (*d*, $^1J(C(sp^2;$ cod),$^{103}Rh)$ = 12.1, olef. C (cod)); 39.5 (*s*, 2 Me_2CH); 30.3 (*s*, allyl. C (cod)); 24.5, 24.0 (2*s*, 2 Me_2CH). Anal. calc. for $C_{24}H_{32}BF_4Rh$ (510.23): C 56.50, H 6.32; found: C 56.31, H 6.56.

[(1,2,5,6-η)-Cycloocta-1,5-diene][(1,2,3,3a,8a-η)-7-isopropyl-4-methylazulene]rhodium(1+) Tetrafluoroborate(1−) ($[Rh^{I}(cod)(\eta^5\text{-}7\text{-isopropyl-4-methylazulene})][BF_4]$; **3f**): M.p. 196.8–198.0°. UV/VIS (CH_2Cl_2): 514.0 (3.83), 356.4 (sh, 3.60), 344.4 (sh, 3.66), 314.0 (sh, 4.12), 302.0 (4.15), 286.8 (sh, 4.31); 281.2 (4.33); min.: 428.2 (3.32), 298.8 (4.14), 254.8 (4.16). ^{1}H-NMR (300 MHz, $CDCl_3$): 8.04 (br. *s*, H–C(8)); 8.00 (br. *d*, $^3J(6,5)$ = 10.9, H–C(6)); 7.73 (*d*, $^3J(5,6)$ = 10.8, H–C(5)); 7.18 (superimp. *td*, $^3J(1,2)$ = 2.9, $^2J(2,^{103}Rh)$ = 2.1, H–C(2)); 6.13 (br. *s*, with f.s., H–C(1), H–C(3)); 5.09, 4.70 (br. 2*s*, olef. H (cod)); 3.21 (*sept.*, ^3J = 6.9, Me_2CH); 2.53 (*s*, Me–C(4)); 2.17–1.91 (*m*, allyl. H (cod)); 1.41 (*d*, ^3J = 6.9, Me_2CH). Coalescence temp.: 259 K, $\Delta\nu$ = 55.33 Hz; 279 K, $\Delta\nu$ = 116.41 Hz. ^{13}C-NMR (75 MHz, $CDCl_3$): 154.8 (*s*, C(4)); 145.1 (*s*, C(7)); 138.4 (*s*, C(5)); 136.3 (*s*, C(6)); 135.3 (*s*, C(8)); 114.1, 112.8 (2*d*, $^1J(3a,^{103}Rh)$ = 2.9, $^1J(8a,^{103}Rh)$ = 3.0, C(3a), C(8a); or *vice versa*); 104.5 (*d*, $^1J(2,^{103}Rh)$ = 4.4, C(2)); 88.8, 87.2 (2*d*, $^1J(1,^{103}Rh) = {}^1J(3,^{103}Rh)$ = 2.9, C(1), C(3)); 82.4, 79.9 (2*d*, $^1J(C(sp^2;$ cod),$^{103}Rh)$ = 12.0, 11.1, olef. C (cod)); 38.4 (*s*, Me_2CH); 31.2, 29.8 (2*s*, allyl. C (cod)); 24.9, 24.3 (2*s*, Me_2CH); 23.8 (*s*, Me–C(4)). Anal. calc. for $C_{22}H_{28}BF_4Rh$ (482.18): C 54.80, H 5.85; found: C 54.69, H 5.80.

[(1,2,5,6-η)-Cycloocta-1,5-diene][(1,2,3,3a,8a-η)-azulene]rhodium(1+) Tetrafluoroborate(1−) ($[Rh^{I}(cod)(\eta^5\text{-azulene})][BF_4]$; **3g**): M.p. 235.0–236.0°. UV/VIS (CH_2Cl_2): 514.6 (3.63), 476 (sh, 3.55), 387 (sh, 3.54), 352 (sh, 3.65), 339 (sh, 3.78), 297 (sh, 4.14), 280 (sh, 4.36), 274.6 (4.40); min.: 431.9 (3.47), 247.7 (4.19). ^{1}H-NMR (300 MHz, $CDCl_3$): 8.14 (*d*, $^3J(4,5) = {}^3J(8,7)$ = 9.7, H–C(4), H–C(8)); 8.10 (*t*, $^3J(6,5) = {}^3J(6,7)$ = 9.9, H–C(6)); 7.79 (*t*, $^3J(5,6) = {}^3J(7,6) = {}^3J(5,4) = {}^3J(7,8)$ = 10.1, H–C(5), H–C(7)); 7.25 (superimp. *td*, $^3J(2,1) = {}^3J(2,3)$ = 3.0, $^2J(2,^{103}Rh)$ = 2.3, H–C(2)); 6.35 (*d*, $^3J(1,2) = {}^3J(3,2)$ = 3.0, H–C(1), H–C(3)); 5.21 (br. *s*, olef. H (cod)). Coalescence temp.: 251 K, $\Delta\nu$ = 75.50. ^{13}C-NMR (75 MHz, $CDCl_3$): 139.1 (*s*, C(6)); 134.5, 134.2 (2*s*, C(4), C(8), C(5), C(7)); 113.9 (*d*, $^1J(3a,^{103}Rh) = {}^1J(8a,^{103}Rh)$ = 3.1, C(3a), C(8a)); 105.0

(*d*, $^1J(2,^{103}Rh) = 4.2$, C(2)); 88.9 (*d*, $^1J(1,^{103}Rh) = {}^1J(3,^{103}Rh) = 4.6$, C(1), C(3)); 81.5 (*m*, olef. C (cod)); 30.3 (*s*, allyl. C (cod)). Anal. calc. for $C_{18}H_{20}BF_4Rh$ (426.07): C 50.74, H 4.73; found: C 50.62, H 4.52.

2.2. *Data of the [Rh^I(nbd)(azulene)] Complex Salts* **4a**, **4b**, *and* **4d**.

[(2,3,5,6-η)-Bicyclo[2.2.1]hepta-2,5-diene][(1,2,3,3a,8a-η)-7-isopropyl-1,4-dimethylazulene]rhodium(1+) Tetrafluoroborate(1−) ([Rh^I(nbd)(η^5-7-isopropyl-1,4-dimethylazulene)][BF_4]; **4a**): M.p. 204.3–206.1°. UV/VIS (CH_2Cl_2): 493.3 (3.53), 369.2 (sh, 3.67), 317.1 (4.17), 305.5 (4.17), 281.5 (4.31); min.: 421.9 (3.39), 309.8 (4.15), 302.0 (4.16), 254.4 (4.18). ^{1}H-NMR (300 MHz, $CDCl_3$): 8.02 (*dd*, $^3J(6,5) = 10.8$, $^4J(6,8) = 1.5$, H–C(6)); 7.94 (*s*, H–C(8)); 7.78 (*d*, $^3J(5,6) = 10.8$, H–C(5)); 7.25 (*d*, $^3J(2,3) = 2.3$, H–C(2)); 6.17 (*d*, $^3J(3,2) = 3.1$, H–C(3)); 4.53, 4.02 (2 br. *s*, olef. H (nbd)); 3.46 (br. *s*, H–C(1)(nbd), H–C(4)(nbd)); 3.30 (*sept.*, $^3J(H,H) = 6.9$, Me_2CH); 2.60 (*s*, Me–C(4)); 2.23 (*s*, Me–C(1)); 1.44, 1.42 (2*d*, $J = 6.9$, Me_2CH); 1.03 (*s*, CH_2(7)(nbd)). Coalescence temp.: 230 K, $\Delta\nu = 186.0$. ^{13}C-NMR (50 MHz, $CDCl_3$): 152.9 (*s*, C(4)); 147.4 (*s*, C(7)); 138.9 (*s*, C(5)); 135.2 (*s*, C(6)); 131.9 (*s*, C(8)); 110.1, 108.7 (*s*, C(3a), C(8a)); 106.3 (*d*, $^1J(2,^{103}Rh) = 5.0$, C(2)); 83.4 (*s*, C(3)); 60.9 (*s*, CH_2(nbd)); 58.1 (*d*, $^1J(C(sp^2;$ nbd),$^{103}Rh) = 8.3$, 2 olef. C (nbd)); 55.3 (*d*, $^1J(C(sp^2;$ nbd),$^{103}Rh) = 8.7$, 2 olef. C (nbd)); 49.2 (*s*, C(1)(nbd), C(4)(nbd); 38.5 (*s*, Me_2CH); 24.7, 24.6 (2*s*, Me_2CH); 24.0 (*s*, *Me*–C(4)); 11.1 (*s*, *Me*–C(1)). Anal. calc. for $C_{22}H_{26}BF_4Rh$ (480.16): C 55.03, H 5.46; found: C 54.86, H 5.29.

[(2,3,5,6-η)-Bicyclo[2.2.1]hepta-2,5-diene][(1,2,3,3a,8a-η)-4,6,8-trimethylazulene]rhodium(1+) Tetrafluoroborate(1−) ([Rh^I(nbd)(η^5-4,6,8-trimethylazulene)][BF_4]; **4b**): M.p. 184.3–185.6°. UV/VIS (CH_2Cl_2): 499.6 (3.64), 350.2 (sh, 3.73), 285.4 (4.31); min.: 412.1 (3.47), 254.0 (4.20). ^{1}H-NMR (300 MHz, $CDCl_3$): 8.71 (*s*, H–C(5), H–C(7)); 7.21 (br. *q*-like, $^3J(2,3) \approx 3$, H–C(2)); 6.20 (*d*, $^3J(1,2) = {}^3J(3,2) = 3.1$, H–C(1), H–C(3)); 4.21 (br. *s*, olef. H (nbd)); 3.43 (br. *s*, H–C(1)(nbd), H–C(4)(nbd)); 2.77 (*s*, Me–C(6)); 2.67 (*s*, Me–C(4), Me–C(8)); 1.01 (*s*, CH_2(7)(nbd)). No coalescence temp. for the olef. δ(H) down to 220 K. ^{13}C-NMR (50 MHz, $CDCl_3$): 154.3 (*s*, C(6)); 149.9 (*s*, C(4), C(8)); 135.7 (*s*, C(5), C(7)); 109.2 (*s*, C(3a), C(8a)); 104.0 (*s*, C(2)); 87.2 (*s*, C(1), C(3)); 60.3 (*s*, CH_2(7)(nbd)); 52.6 (*d*, $^1J(C(sp^2;$ nbd),$^{103}Rh) = 9.1$, olef. C (nbd)); 49.1 (*s*, C(1)(nbd), C(4)(nbd)); 29.8 (*s*, *Me*–C(6)); 25.6 (*s*, *Me*–C(4), *Me*–C(8)). Anal. calc. for $C_{20}H_{22}BF_4Rh$ (452.11): C 53.13, H 4.91; found: C 52.91, H 4.72.

[(2,3,5,6-η)-Bicyclo[2.2.1]hepta-2,5-diene][(1,2,3,3a,8a-η)-5,7-dimethylazulene]rhodium(1+) Tetrafluoroborate(1−) ([Rh^I(nbd)(η^5-5,7-dimethylazulene)][BF_4]; **4d**): M.p. 205.6–207.1°. UV/VIS (CH_2Cl_2): 492.8 (3.67), 355.2 (sh, 3.79), 280.0 (sh, 4.43); min.: 419.1 (3.43), 252.4 (4.28). ^{1}H-NMR (300 MHz, $CDCl_3$): 8.03 (*s*, H–C(4), H–C(8)); 7.97 (*s*, H–C(6)); 7.18 (*q*-like, $^3J(2,1) \approx {}^3J(2,3) \approx 2.4$, H–C(2)); 6.03 (*d*, $^3J(1,2) = {}^3J(3,2) = 2.8$, H–C(1), H–C(3)); 4.66 (br. *s*, olef. H (nbd)); 3.39 (br. *s*, H–C(1)(nbd), H–C(4)(nbd)); 2.79 (*s*, 2 Me); 1.06 (*s*, CH_2(7) (nbd)). No coalescence temp. for the olef. δ(H) down to 220 K. ^{13}C-NMR (50 MHz, $CDCl_3$): 143.9 (*s*, C(5), C(7)); 143.3 (*s*, C(6)); 134.6 (*s*, C(4), C(8)); 112.3 (*s*, C(3a), C(8a)); 105.2 (*s*, C(2)); 83.4 (*s*, C(1), C(3)); 62.5 (*s*, CH_2(7) (nbd)); 56.6 (*d*, $^1J(C(sp^2;$ nbd),$^{103}Rh) = 7.8$, olef. C (nbd)); 49.1 (*s*, C(1)(nbd), C(4)(nbd)); 27.4 (*s*, 2 Me). Anal. calc. for $C_{19}H_{20}BF_4Rh$ (438.08): C 52.09, H 4.60; found: C 51.87, H 4.48.

2.3. *[(1,2,5,6-η)-Cycloocta-1,5-diene][(1,2,3,3a,8a-η)-7-isopropyl-1,4-dimethylazulene]iridium(1+) Tetrafluoroborate(1−)* [Ir^I(cod)(η^5-7-isopropyl-1,4-dimethylazulene)][BF_4]; **5a**): M.p. >290°. UV/VIS (CH_2Cl_2): 538.0 (3.68), 434.0 (3.65), 364.4 (sh, 3.71), 304.4 (4.16), 291.6 (4.25); min.: 482.6 (3.58), 400.4 (3.57), 255.6 (4.09). ^{1}H-NMR (300 MHz, $CDCl_3$): 8.38 (*dd*, $^3J(6,5) = 11.0$, $^4J(6,8) = 1.6$, H–C(6)); 7.94 (*d*, $^4J(8,6) = 1.6$, H–C(8)); 7.54 (*d*, $^3J(5,6) = 11.0$, H–C(5)); 6.78 (*d*, $^3J(2,3) = 3.1$, H–C(2)); 6.16 (*d*, $^3J(3,2) = 2.9$, H–C(3)); 5.33, 4.59 (2 br. *s*, olef. H (cod)); 3.26 (*sept.*, $^3J = 6.9$, Me_2CH); 2.39 (*s*, Me–C(4)); 2.35 (*s*, Me–C(1)); 2.05–1.92 (*m*, allyl. H (cod)); 1.39 (*d*, $^3J = 6.9$, Me_2CH). Coalescence temp.: 254 K, $\Delta\nu = 145.67$ Hz; 255 K, $\Delta\nu = 232.16$ Hz. NOE (400 MHz, $CDCl_3$): 6.78 (H–C(2)) → 6.16 (*m*, H–C(3)), 2.35 (*m*, Me–C(1)). Anal. calc. for $C_{23}H_{30}BF_4Ir$ (585.52): C 47.18, H 5.16; found: C 46.94, H 5.06.

REFERENCES

[1] A. J. Rippert, A. Linden, H.-J. Hansen, *Helv. Chim. Acta* **1993**, *76*, 2876.
[2] R. R. Schrock, J. A. Osborn, *J. Am. Chem. Soc.* **1971**, *93*, 3089.
[3] P. Mohler, A. J. Rippert, H.-J. Hansen, *Helv. Chim. Acta* **2000**, *83*, 258.
[4] W. J. Hälg, L. R. Oehrström, H. Rüegger, L. M. Venanzi, T. Gerfin, V. Gramlich, *Helv. Chim. Acta* **1993**, *76*, 788; W. J. Hälg, L. R. Oehrström, H. Rüegger, L. M. Venanzi, *Magn. Reson. Chem.* **1993**, *31*, 677.
[5] P. A. Plattner, *Helv. Chim. Acta* **1941**, *24*, 283E.
[6] E. Heilbronner, in 'Non-Benzenoid Aromatic Compounds', Ed. D. Ginsburg, Interscience Publ., Inc., New York, 1959, p. 246; F. Gerson, E. Heilbronner, *Helv. Chim. Acta* **1959**, *42*, 1877.

[7] F. Gerson, M. Scholz, H.-J. Hansen, P. Uebelhart, *J. Chem. Soc., Perkin Trans. 2* **1995**, 215.
[8] P. Pyykkö, *Chem. Rev.* **1988**, *88*, 563.
[9] F. A. L. Anet, L. Kozerski, *J. Am. Chem. Soc.* **1973**, *95*, 3407.
[10] N. L. Allinger, J. T. Sprague, *Tetrahedron* **1975**, *31*, 21; N. L. Allinger, J. F. Viskocil Jr., U. Burkert, Y. Yuh, *Tetrahedron* **1976**, *32*, 33; W. R. Rocha, W. B. De Almeida, *J. Comput. Chem.* **1997**, *18*, 254; W. R. Rocha, W. B. De Almeida, *Vibrat. Spectrosc.* **1997**, *13*, 213.
[11] G. Giordano, R. H. Crabtree, *Inorg. Synth.* **1990**, *28*, 88.
[12] E. W. Abel, M. A. Bennett, G. Wilkinson, *J. Chem. Soc.* **1959**, 3178.
[13] J. L. Herde, J. C. Lambert, C. V. Senoff, *Inorg. Synth.* **1974**, *15*, 18.
[14] Y. Chen, H.-J. Hansen, *Helv. Chim. Acta* **1993**, *76*, 168; Y. Chen, Ph. D. Thesis, University of Zurich, 1993.
[15] A. Magnussen, P. Uebelhart, H.-J. Hansen, *Helv. Chim. Acta* **1993**, *76*, 2887.
[16] D. N. Laikov, *Chem. Phys. Lett.* **1997**, *281*, 151.
[17] J. P. Perdew, K. Burke, M. Ernzerhof, *Phys. Rev. Lett.* **1996**, *77*, 3865.

Received March 20, 2002